JOURNAL OF SOLID STATE CHEMISTRY 62, 16–25 (1986)

# The Crystal Structure and Magnetic Properties of the Synthetic Langbeinite $KBaFe_2(PO_4)_3$

PETER D. BATTLE[1]

*Department of Inorganic and Structural Chemistry, The University, Leeds LS2 9JT, England*

ANTHONY K. CHEETHAM AND WILLIAM T. A. HARRISON

*Chemical Crystallography Laboratory, 9 Parks Road, Oxford OX1 3PD, England*

AND GARY J. LONG

*Department of Chemistry, University of Missouri-Rolla, Rolla, Missouri 65401, and the Department of Physics, Liverpool University, Liverpool L69 3BX, England*

Received February 27, 1985; in revised form July 17, 1985

Powder neutron diffraction data have been used to refine the crystal structure of $KBaFe_2(PO_4)_3$ at 4.2 K; space group $P2_13$, $a_0 = 9.8732(1)$ Å. The material is isostructural with the mineral langbeinite, having two crystallographically distinct, octahedrally coordinated $Fe^{3+}$ ions in the asymmetric unit. Mössbauer effect spectroscopy and magnetic susceptibility measurements show that $KBaFe_2(PO_4)_3$ orders as an *L*-type ferrimagnet with $3.9 < T_C < 4.2$ K. The variation of $H_{int}$ has been monitored by Mössbauer spectroscopy in the temperature range $1.3 < T < 4.2$ K. © 1986 Academic Press, Inc.

## Introduction

We have recently reported the structural and magnetic properties of the *L*-type ferrimagnets $Fe_2(SO_4)_3$ (*1*) and $Fe_2(MoO_4)_3$ (*2*) which have a garnet-related structure consisting of an infinite network of $FeO_6$ octahedra sharing corners with $XO_4$ tetrahedra ($X$ = S or Mo). The magnetic superexchange takes place along pathways of the form Fe–O–*X*–O–Fe and leads to Curie temperatures of 28 and 12 K in the sulfate and molybdate, respectively. The ferrimagnetism arises because, although all the superexchange interactions between $Fe^{3+}$ : $d^5$ ions are inherently antiferromagnetic, the monoclinic symmetry of the structures requires that there are two crystallographically distinct iron sites in $Fe_2(SO_4)_3$ and four in $Fe_2(MoO_4)_3$. The different sites experience slightly different molecular fields below the magnetic ordering temperature and hence the dependence of sublattice magnetization on temperature differs for each site, leading to a small, uncompensated magnetization in the temperature range $0 < T < T_c$ (*3*). The effect can be detected ex-

[1] Author to whom correspondence should be addressed.

0022-4596/86 $3.00

perimentally by Mössbauer spectroscopy, where the observed spectrum consists of two or more overlapping sextets, one from each site. The inverse magnetic susceptibility of an *L*-type ferrimagnet shows a sharp fall at $T_c$ but then increases again as the sublattice magnetizations approach the same saturation value at absolute zero.

The factors which determine the Curie temperatures of $Fe_2(SO_4)_3$ and $Fe_2(MoO_4)_3$ have been discussed previously (*2*). They include the length of the superexchange pathway, which is governed by the size of *X*, and the nature of the bonding in the $XO_4$ group, which is governed by the electronegativity of *X*. In order to develop this study further, we have prepared and investigated the material $KBaFe_2(PO_4)_3$ (*4*), which is isostructural with the mineral langbeinite, $K_2Mg_2(SO_4)_3$ (*5*) and thus has two crystallographically distinct $Fe^{3+}$ sites in a cubic structure. It is intermediate between the garnet structure, $A_3M_2(XO_4)_3$ and the monoclinic ferric sulfate type, $M_2(XO_4)_3$. The material affords us the opportunity to compare superexchange through phosphate groups with that through molybdate and sulfate, but unfortunately, the nature of *X* is not the only modification to the structure, as two of three previously vacant *c* sites in the distorted garnet structure are now occupied by the cations, $K^+$ and $Ba^{2+}$. These ions might be expected to compete for the anion charge density which will not then be available for superexchange interactions, thus lowering the Curie temperature. Electronegativity arguments would lead us to predict that the superexchange through phosphate would be stronger than that through molybdate but weaker than that through sulfate. Size arguments lead to the same conclusion. In order to test these predictions we have studied $KBaFe_2(PO_4)_3$ by Mössbauer spectroscopy and magnetic susceptibility techniques. We have also carried out neutron diffraction experiments to obtain an accurate picture of the environments of the $Fe^{3+}$ ions, and to ascertain whether the potassium and barium cations are ordered or disordered. The results of the diffraction experiments have been compared to predictions made by lattice energy calculations.

## Experimental

A polycrystalline sample of $KBaFe_2(PO_4)_3$ was prepared by firing a stoichiometric mixture of potassium and barium carbonates, ferric oxide, and ammonium dihydrogen phosphate for 72 hr at a temperature of 1100°C in a platinum crucible. Guinier photographs and analytical electron microscopy indicated that the product was an homogeneous single phase. Powder neutron diffraction data were collected at 4.2 K using the diffractometer D1a at ILL Grenoble, France. A mean neutron wavelength of 1.909 Å was used to collect data at $2\theta$ intervals of 0.05° in the angular range $20° < 2\theta < 158°$ with a monitor count of $3 \times 10^4$ neutrons per point. Magnetic susceptibility measurements were made on an Oxford Instruments Faraday balance using a magnetic field of 9.95 kG and a field gradient of 122 G $cm^{-1}$.

The Mössbauer effect absorber was prepared by mixing finely powdered $KBaFe_2(PO_4)_3$ with Vaseline to remove as far as possible any potential crystallite orientation effects and contained ca. 54 mg/$cm^2$. The spectra were obtained on a Harwell constant acceleration spectrometer which used a room-temperature rhodium-matrix source and was calibrated at room temperature with natural $\alpha$-iron foil. Liquid-helium and subhelium temperature spectra were obtained in a cryostat in which the sample was placed directly into liquid helium. The sample temperature was measured by determining the vapor pressure of helium gas in equilibrium with the liquid helium. The variation in the sample temperature during the accumulation of the Mössbauer spec-

TABLE I

ATOMIC COORDINATES FOR $KBaFe_2(PO_4)_3$ AT 4.2 K

| Atom | Site | $x$ | $y$ | $z$ |
|---|---|---|---|---|
| K/Ba(1) | 4*a* | 0.0672(4) | 0.0672(4) | 0.0672(4) |
| K/Ba(2) | 4*a* | 0.2959(5) | 0.2959(5) | 0.2959(5) |
| Fe(1) | 4*a* | 0.5855(2) | 0.5855(2) | 0.5855(2) |
| Fe(2) | 4*a* | 0.8526(2) | 0.8526(2) | 0.8526(2) |
| P | 12*b* | 0.6263(4) | 0.4606(3) | 0.2724(5) |
| O(1) | 12*b* | 0.6531(3) | 0.5012(4) | 0.4185(4) |
| O(2) | 12*b* | 0.7607(4) | 0.4845(4) | 0.1993(4) |
| O(3) | 12*b* | 0.5796(4) | 0.3160(4) | 0.2594(4) |
| O(4) | 12*b* | 0.5245(4) | 0.5537(4) | 0.2031(4) |

*Note.* The following neutron scattering lengths were used: $b_{Ba} = 0.52$, $b_k = 0.37$, $b_{Fe} = 0.96$, $b_p = 0.51$, $b_o = 0.58 \times 10^{-14}$m.

trum is indicated in the brackets in the figures and in Table III. In other words the temperature ranged from 2.33 to 2.29 K for the spectrum obtained at 2.31(2) K for a percentage change of 1.7. The largest such change is 3.1% at 1.30(2) K.

## Results

### *Neutron Diffraction*

The neutron diffraction data collected at 4.2 K could be indexed in the same cubic space group, $P2_13$, as has been reported in a previous room temperature study (*4*) of $KBaFe_2(PO_4)_3$. The diffraction pattern was analyzed using the Rietveld profile analysis technique (*6*), taking the coordinates of $K_2Mg_2(SO_4)_3$ (*5*) as a starting model for the structure. There was no evidence to suggest that the material is magnetically ordered at 4.2 K. The intensities of 224 reflections, distributed over 2760 profile points, were used to refine 19 atomic parameters and the usual profile parameters, leading to a final weighted profile $R$ factor of 9.7%. The final atomic coordinates are listed in Table I and selected bond lengths and bond angles are presented in Table II. The unit cell parameter refined to a value of 9.8732(1) Å are the overall isotropic $B$ factor to 0.02(2) Å$^2$. Here and throughout this paper the number in brackets is the estimated standard deviation in the last figure. The observed and calculated diffraction profiles are drawn in Fig. 1. Models in which the potassium and barium ions were partially or completely ordered over the two sites gave less satisfactory fits than the disordered model described in Table 1.

### *Magnetic Susceptibility*

The low temperature behavior of the inverse susceptibility of $KBaFe_2(PO_4)_3$ is shown in Fig. 2. It is apparent that below 5 K the curve deviates from a Curie–Weiss behavior in a manner similar to that found in $Fe_2(SO_4)_3$ and $Fe_2(MoO_4)_3$ (*1*, *2*). This deviation is due to the onset of magnetic ordering.

### *Lattice Energy Calculations*

The atomic coordinates listed in Table I were used to calculate (*7*) the lattice energy of $KBaFe_2(PO_4)_3$, assuming that the potassium and barium ions each occupied a distinct 4*a* site. The values (22.446 and 22.464 MJ mole$^{-1}$) calculated for the two possible

TABLE II

BOND LENGTHS (IN Å) AND BOND ANGLES (IN DEGREES) FOR $KBaFe_2(PO_4)_3$ AT 4.2 K

| | | | |
|---|---|---|---|
| Fe(1)–O(1) | 1.964(8) (×3) | P–O(1) | 1.52(1) |
| Fe(1)–O(2) | 2.014(8) (×3) | P–O(2) | 1.53(1) |
| Fe(2)–O(3) | 2.016(8) (×3) | P–O(3) | 1.51(1) |
| Fe(2)–O(4) | 2.012(8) (×3) | P–O(4) | 1.52(1) |
| O(1)–Fe(1)–O(1)′ | 94.3 | O(1)–P–O(2) | 104.9 |
| O(2)–Fe(1)–O(2)′ | 91.6 | O(1)–P–O(3) | 112.5 |
| O(1)–Fe(1)–O(2) | 80.9 | O(1)–P–O(4) | 112.5 |
| O(1)–Fe(1)–O(2)′ | 170.9 | O(2)–P–O(3) | 111.9 |
| O(1)–Fe(1)–O(2)″ | 93.8 | O(2)–P–O(4) | 105.5 |
| | | O(3)–P–O(4) | 109.4 |
| O(3)–Fe(2)–O(3)′ | 92.9 | | |
| O(4)–Fe(2)–O(4)′ | 88.1 | | |
| O(3)–Fe(2)–O(4) | 90.4 | | |
| O(3)–Fe(2)–O(4)′ | 88.5 | | |
| O(3)–Fe(2)–O(4)″ | 176.4 | | |

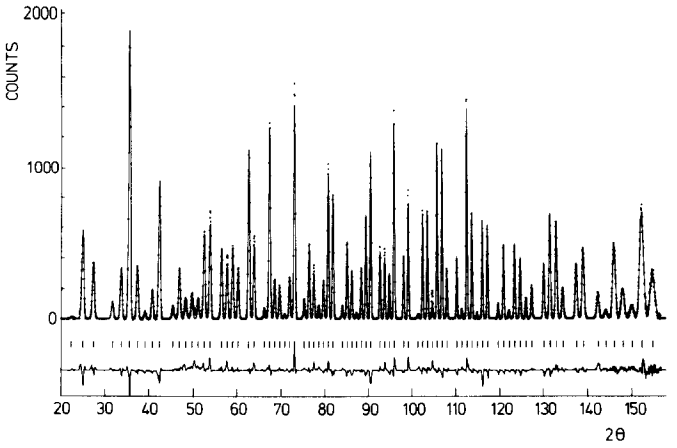


FIG. 1. The observed (···), calculated (—), and difference profiles for $KBaFe_2(PO_4)_3$ at 4.2 K. Reflection positions are marked.

arrangements differ by so little that we would expect to observe a disordered arrangement, as is indicated by the neutron diffraction results. A disordered arrangement could be anticipated in view of the similar ionic radii of $K^+$ and $Ba^{2+}$.

### *Mössbauer Spectroscopy*

The Mössbauer effect data were initially analyzed using standard least-squares minimization techniques to evaluate the hyperfine spectral parameters reported in Table III. The observed and calculated spectra are shown in Figs. 3–5 for temperatures between 4.2 and 1.3 K. In the data analysis, two magnetic sextets of equal area, one for each crystallographic site, were fitted to the observed spectra on the basis of an adjustable isomer shift, $\delta$, internal hyperfine field, $H_{int}$, quadrupole shift, QS, and linewidth, $\Gamma$, which was the width of the inner magnetic lines, lines 3 and 4. The linewidths of lines 2 and 5 were constrained to be $\Gamma + 0.5\Delta\Gamma$ and those of lines 1 and 6 to be $\Gamma + \Delta\Gamma$, where $\Delta\Gamma$ was determined from preliminary fits and was not refined. The relative areas of the lines in each of the two sextets were constrained to be in the ratio 3 : 2 : 1 : 1 : 2 : 3 as is required for an unoriented powder sample. The results indicated that at 4.2 K $KBaFe_2(PO_4)_3$ has no long-range magnetic order and the spectrum is a simple quadrupole doublet with hyperfine parameters typical of high-spin iron(III) in an approximately octahedral coordination geometry. Between 4.2 K and 3.9 K the compound begins to undergo long-range magnetic ordering and upon further cooling the spectrum broadens and eventually shows the sextet of lines expected for a material exhibiting long-range magnetic order.

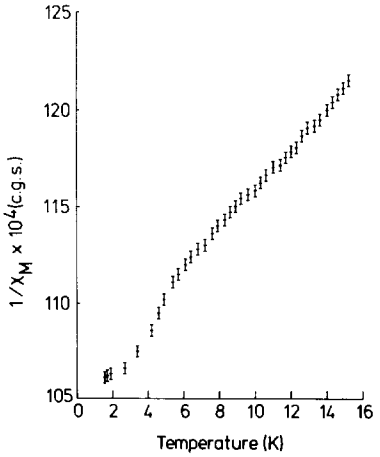


FIG. 2. The inverse molar magnetic susceptibility of $KBaFe_2(PO_4)_3$ as a function of temperature.

TABLE III

MÖSSBAUER EFFECT SPECTRAL PARAMETERS[a]

| T (K) | Site 1 | | | | | Site 2 | | | | | Area[b] | $\chi^2$ |
|---|---|---|---|---|---|---|---|---|---|---|---|---|
| | δ | QS | H | Γ | ΔΓ | δ | QS | H | Γ | ΔΓ | | |
| 1.30(2) | 0.59 | 0.00 | 516 | 0.41 | 0.10 | 0.59 | −0.01 | 494 | 0.47 | 0.34 | 23.5 | 1.89 |
| 1.51(2) | 0.59 | 0.00 | 511 | 0.49 | 0.14 | 0.58 | −0.01 | 484 | 0.63 | 0.46 | 19.7 | 3.00 |
| 2.04(2) | 0.60 | −0.01 | 494 | 0.48 | 0.31 | 0.58 | 0.00 | 454 | 0.67 | 0.63 | 24.0 | 1.23 |
| 2.31(2) | 0.58 | 0.00 | 468 | 0.62 | 0.58 | 0.60 | 0.00 | 412 | 1.34 | 0.52 | 19.5 | 2.56 |
| 2.53(1) | 0.57 | 0.00 | 449 | 0.73 | 0.75 | 0.61 | 0.00 | 381 | 1.44 | 1.00 | 20.5 | 1.84 |
| 2.76(1) | 0.56 | 0.00 | 412 | 0.87 | 1.11 | 0.58 | −0.01 | 312 | 2.48 | 0.84 | 22.8 | 1.71 |
| 3.01(1) | 0.57 | 0.00 | 374 | 1.03 | 1.63 | 0.57 | 0.00 | 269 | 2.66 | 0.45 | 21.9 | 1.69 |
| 3.249(5) | 0.57 | 0.00 | 320 | 1.29 | 2.22 | 0.57 | 0.00 | 217 | 2.35 | 0.78 | 22.1 | 1.40 |
| 3.50(1) | 0.57 | 0.00 | 180 | 2.58 | 1.98 | 0.57 | 0.00 | 120 | 3.29 | 0.82 | 21.0 | 1.07 |
| 3.73(1) | 0.57 | 0.00 | 93 | 1.15 | 2.37 | 0.58 | 0.03 | 55 | 0.96 | 2.36 | 23.0 | 0.86 |
| 3.94(2) | 0.57 | 0.00 | 25 | 0.73 | 0.73 | 0.57 | 0.00 | 15 | 0.73 | 0.73 | 20.3 | 1.14 |
| 4.20(5) | 0.57 | 0.42[c] | — | 0.62 | — | | | | | | 18.4 | 1.00 |
| 78.0 | 0.55 | 0.31[c] | — | 0.38 | — | | | | | | 18.2 | 1.11 |

[a] All data in mm/s relative to room temperature natural α-iron foil except the internal field which is in kOe.
[b] Absolute area in mm/s percentage effect.
[c] The quadrupole interaction, $\Delta E_Q$.

At all temperatures the refined values of the isomer and quadrupole shifts remain typical of octahedral, high-spin $Fe^{3+}$ but the linewidths calculated for the two sites in this model are unusually large and surprisingly different at temperatures between the Curie point and 1.30 K. Specifically, the linewidths associated with site 2 (Table III) are often twice as great as those associated with site 1. This result was surprising in view of the apparently similar environments of the two sites and we consequently reanalyzed our data using the Window method (8). This technique calculates the function $p(H)$ vs $H$ where $p(H)$ is proportional to the number of $Fe^{3+}$ sites which experience an internal hyperfine field of between $H$ and $H + dH$ kOe. The linewidth is held constant during this analysis. The calculated field distribution (Fig. 6) clearly has two maxima in the temperature range $1.5 < T < 3$ K and this justifies the original decision to fit our data with two magnetic sextets.

## Discussion

The width of the observed Mössbauer effect absorption maxima below $T_c$ stems from many sources; first, the spectrum consists of two overlapping sextets, one associated with each of the two crystallographically distinct $Fe^{3+}$ sites, and each of these sextets is itself broadened by a temperature dependent magnetic relaxation process and by the variation in electric field gradient which is generated by the disorder on the K/Ba sublattice. The disorder will also cause local variations in $H_{int}$ which further broaden the spectra. The geometries of the two $FeO_6$ octahedra must be sufficiently different for the interaction with the K/Ba sublattice to be more significant on site 2 than on site 1, hence the larger value at the former site. The structure of $KBaFe_2(PO_4)_3$ consists of an infinite network of distorted $FeO_6$ octahedra and $PO_4$ tetrahedra. The latter are made up of P–O bonds varying in length betwen 1.51(1) and 1.53(1) Å, ap-

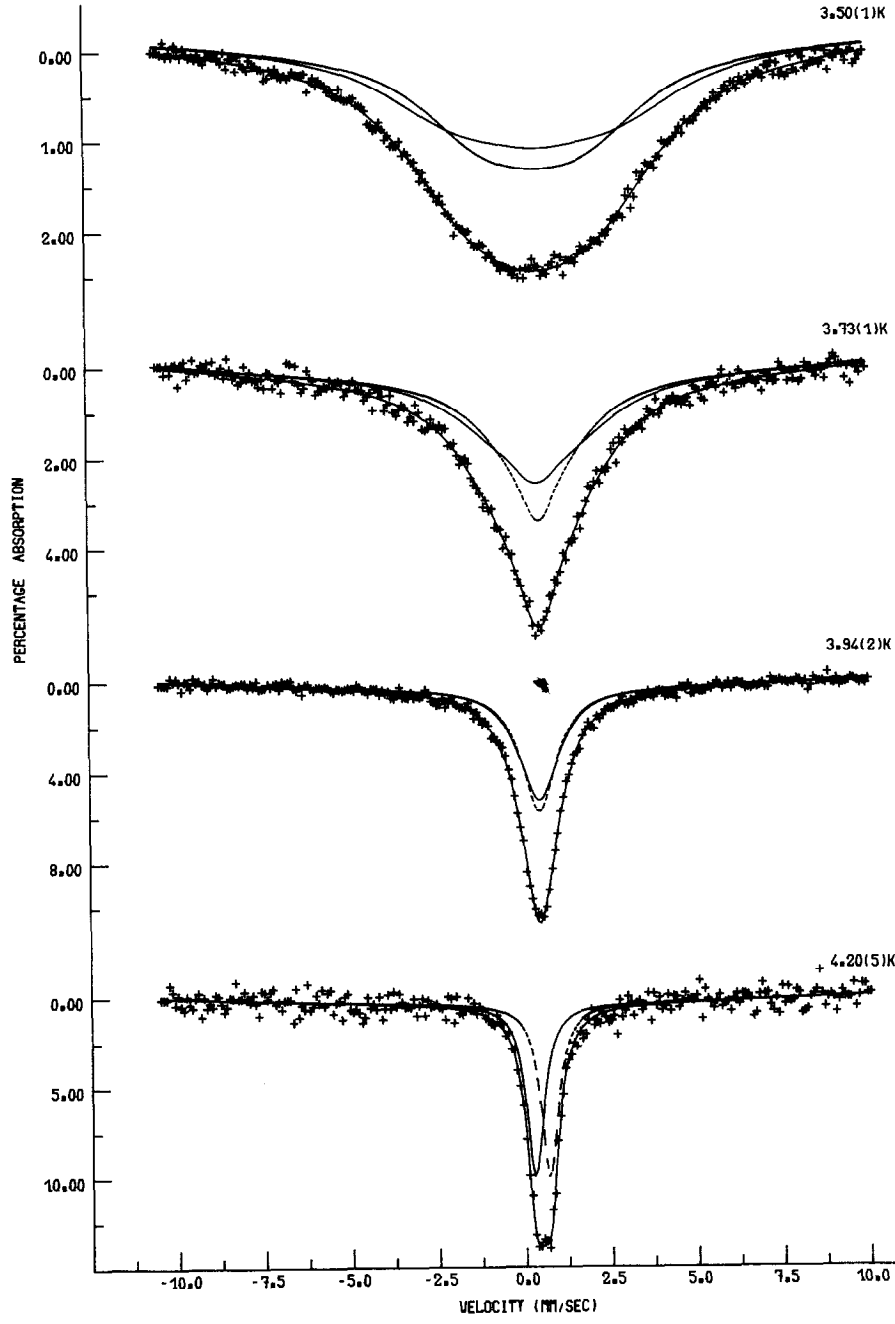


FIG. 3. The observed and calculated Mössbauer effect spectra of $KBaFe_2(PO_4)_3$ in the temperature range $3.5 \leqq T \leqq 4.2$ K.

proximately the same degree of variation as was found in the $SO_4^{2-}$ tetrahedra in $Fe_2(SO_4)_3$ (*1*), while the two $FeO_6$ octahedra have bond lengths that vary between 1.964(8) and 2.014(8) Å for Fe(1) and between 2.012(8) and 2.016(8) Å for Fe(2). The environment around Fe(1) is thus distorted significantly more than that around

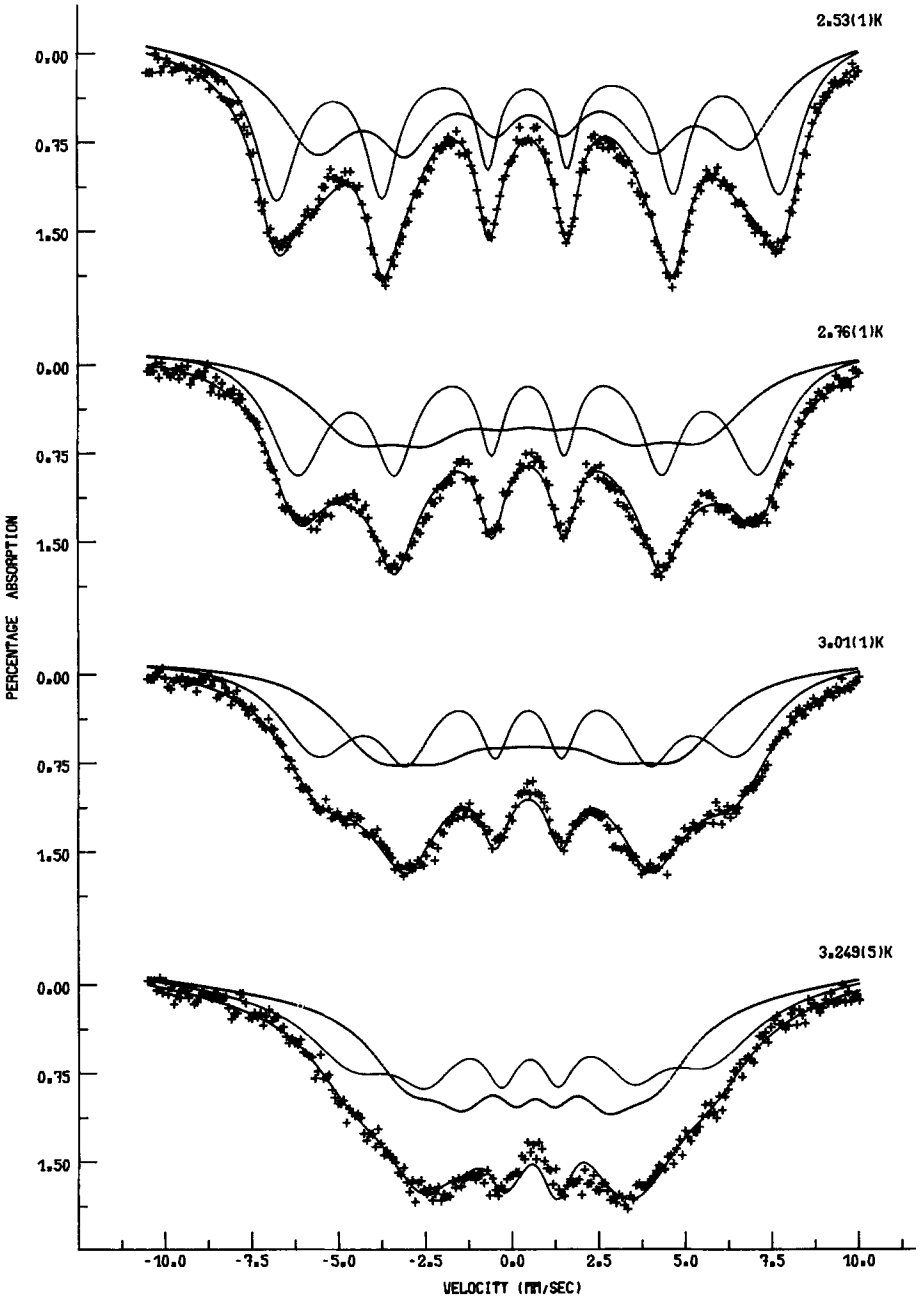


FIG. 4. The observed and calculated Mössbauer effect spectra of $KBaFe_2(PO_4)_3$ in the temperature range $2.5 < T < 3.5$ K.

Fe(2), and this difference is consistent with the explanation of the Mössbauer linewidths which was offered above. The coordination around the K/Ba sites may be described as a distorted, tricapped prism, i.e. 9-coordination rather than the 12-coordination found for the corresponding sites in the garnet structure.

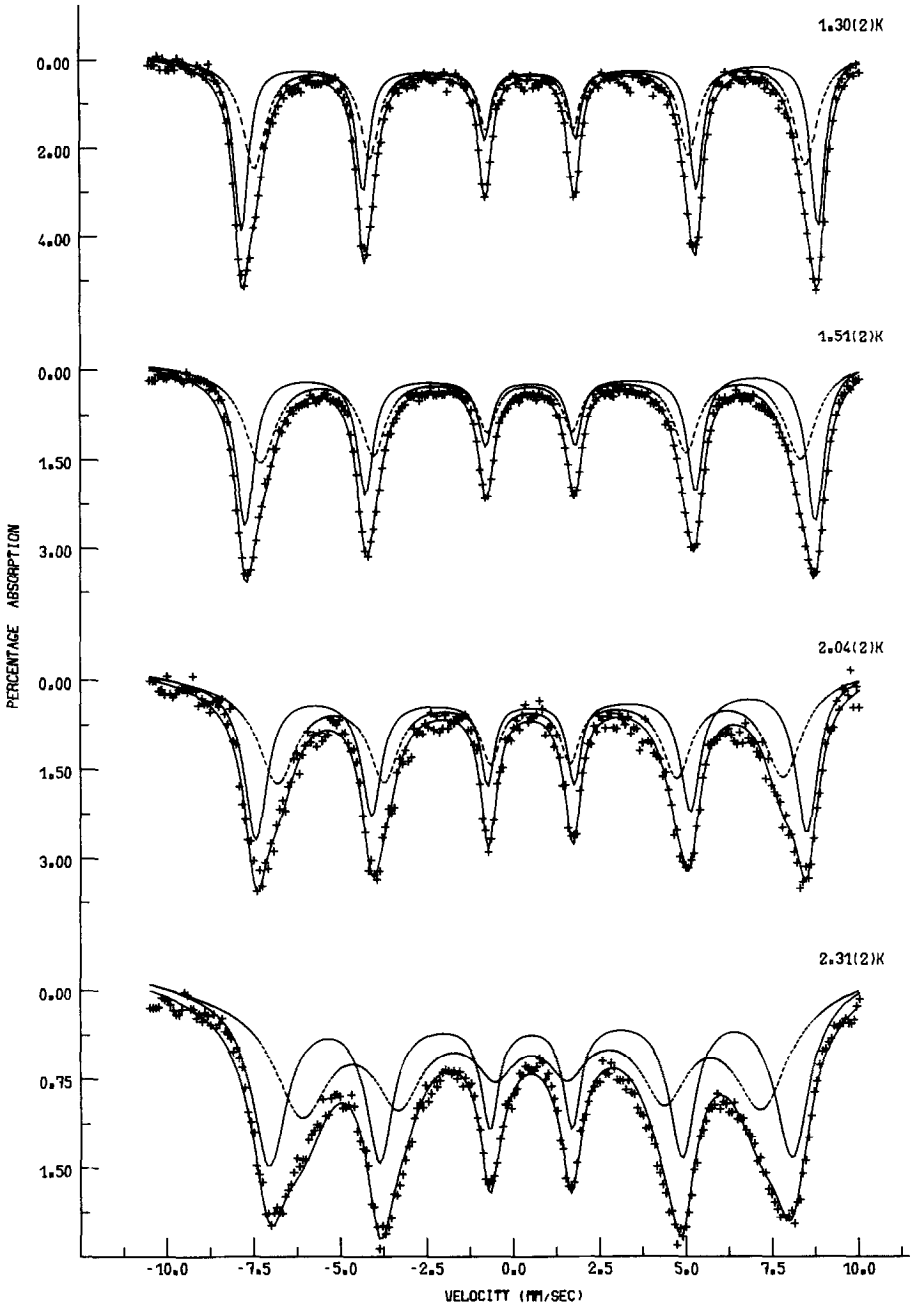


FIG. 5. The observed and calculated Mössbauer effect spectra of $KBaFe_2(PO_4)_3$ in the temperature range $1 < T < 2.5$ K.

Both Mössbauer spectroscopy and neutron diffraction indicate that $KBaFe_2(PO_4)_3$ is paramagnetic at 4.2 K, although the magnetic susceptibility data suggest that some short range order may be present at this temperature. The different $H_{int}$ values calculated for sites 1 and 2 (Table III) suggest that the material orders as an *L*-type ferri-

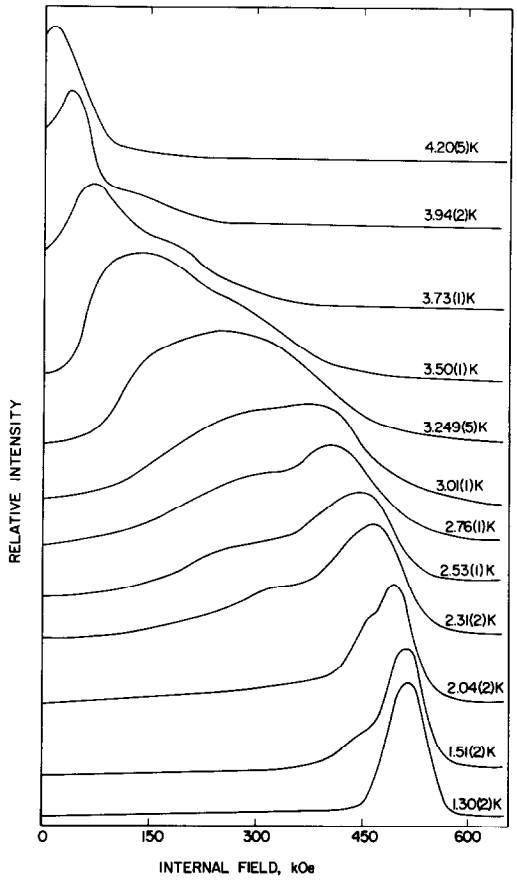


FIG. 6. The distribution of $H_{int}$ for $KBaFe_2(PO_4)_3$ as a function of temperature and $H_{int}$.

magnet with a transition temperature of between 4.2 and 3.94(2) K and the shape of the $1/\chi$ vs $T$ plot (Fig. 2) is also consistent with the ordered state being an $L$-type ferrimagnet. The approximately zero quadrupole shift in the magnetic spectra and the nonzero quadrupole interaction in the paramagnetic spectra indicate that the angle between the principal axis of the EFG tensor and the easy axis of magnetization is approximately 54.7° for each site. The Curie temperature is thus lower than that of both $Fe_2(SO_4)_3$ and $Fe_2(MoO_4)_3$, and not intermediate between the two as might have been predicted on the basis of the arguments given above. It is also lower that the Neel temperature of $FePO_4$ (*9*). We account for this by postulating that the presence of the potassium and barium ions in the 9-coordinate site has a significant effect on the magnetic properties of the $Fe_2(XO_4)_3$ framework, a conclusion which is supported by the unusually broad spectra observed below $T_c$ in $KBaFe_2(PO_4)_3$ but not in either $Fe_2(SO_4)_3$ or $Fe_2(MoO_4)_3$. There may be two contributions to this effect; firstly the $K^+$ and $Ba^{2+}$ ions will compete for the negative charge density on the phosphate ions, thus rendering part of this density unavailable for superexchange interactions and hence lowering the Curie temperature. This effect will occur irrespective of whether the $K^+$ and $Ba^{2+}$ are disordered. The second effect will only occur when the 9-coordinate cations are disordered, as they are in $KBaFe_2(PO_4)_3$. In that case the $Fe^{3+}$ ions will experience a random component in the exchange potential throughout the structure and this variation may be responsible, to some extent, for the depression of the Curie point of $KBaFe_2(PO_4)_3$. The data in Table III suggest that the internal hyperfine fields are not saturated at 1.3 K but the values of 516 kOe (site 1) and 494 kOe (site 2) are typical of $Fe^{3+}$ in an antiferromagnetic material with a significant covalent component in the bonding at the iron site.

## Acknowledgments

We thank the SERC and ILL Grenoble for the provision of neutron facilities. P.D.B. is grateful to the CEGB for financial suport during the early part of this work and W.T.A.H. thanks the SERC for a Studentship. G.J.L. thanks the SERC for a Visiting Research Fellowship during a sabbatical stay at Liverpool University and the Petroleum Research Fund for their partial support of this work through Grant 13485-AC3,5. Further we thank NATO for a cooperative scientific research grant between the University of Missouri–Rolla and Oxford University.

## References

1. G. J. LONG, G. LONGWORTH, P. D. BATTLE, A. K. CHEETHAM, R. V. THUNDATHIL AND D. BEVERIDGE, *Inorg. Chem.* **18**, 624 (1979).

2. P. D. BATTLE, A. K. CHEETHAM, G. J. LONG, AND G. LONGWORTH, *Inorg. Chem.* **21,** 4223 (1982).
3. L. NEEL. *Ann. Phys.* [12] **3,** 137 (1948).
4. R. MASSE, *Bull. Soc. Franc. Min. Cryst.* **95,** 405 (1972).
5. A. ZEMANN AND J. ZEMANN, *Acta Crytallogr.* **10,** 409 (1957).
6. H. M. RIETVELD, *J. Appl. Crystallogr.* **2,** 65 (1969).
7. W. VAN GOOL AND A. G. PIKEN, *J. Mater. Sci.* **4,** 95 (1969).
8. B. WINDOW, *J. Phys. E:Sci. Inst.* **4,** 401 (1971).
9. P. D. BATTLE, A. K. CHEETHAM, C. GLEITZER, W. T. A. HARRISON, G. J. LONG AND G. LONGWORTH, *J. Phys. C: Solid State Phys.* **15,** L919 (1982).